# Role of Soil Thermal Inertia in Surface Temperature and Soil Moisture-Temperature Feedback

F. Cheruy, Jean-Louis Dufresne, S. Aït Mesbah, J. y Grandpeix, F. Wang

AGU PUBLICATIONS

Journal of Advances in Modeling Earth Systems

RESEARCH ARTICLE
10.1002/2017MS001036

# Role of Soil Thermal Inertia in Surface Temperature and Soil Moisture-Temperature Feedback

F. Cheruy[1], J. L. Dufresne[1], S. Aït Mesbah[1], J. Y. Grandpeix[1], and F. Wang[1]

[1]CNRS/IPSL/LMD, Université Pierre et Marie Curie, Paris, France

**Key Points:**
- A conceptual model is developed to compute the sensitivity of the climatological surface temperature to the soil thermal inertia
- The only regions where the thermal inertia has a limited impact are the moist regions
- A new moisture-related negative feedback is identified

**Correspondence to:**
F. Cheruy,
cheruy@lmd.jussieu.fr

**Citation:**
Cheruy, F., Dufresne, J. L., Aït Mesbah, S., Grandpeix, J. Y., & Wang, F. (2017). Role of soil thermal inertia in surface temperature and soil moisture-temperature feedback. *Journal of Advances in Modeling Earth Systems*, *9*, 2906–2919. https://doi.org/10.1002/2017MS001036

Received 3 MAY 2017
Accepted 30 OCT 2017
Accepted article online 3 NOV 2017
Published online 14 DEC 2017



**Abstract** A conceptual model based on the surface energy budget is developed to compute the sensitivity of the climatological mean diurnal amplitude and mean daily surface temperature to the soil thermal inertia. It uses the diurnal amplitude of the net surface radiation, the sensitivity of the turbulent fluxes to the surface temperature and the soil thermal inertia. Its performance is evaluated globally with numerical simulations using the atmospheric and the land surface modules of a state-of-the-art climate model. The only regions where the thermal inertia has a limited impact are the moist regions. In dry areas, together with the stability of the boundary layer it plays a major role. It also has a significant impact at high and midlatitudes especially in winter when the turbulent fluxes are weak. In semiarid regions, the soil moisture exhibits a high day-to-day variability strongly correlated to the evaporation and the day-to-day variability of the surface temperature is generally explained by the soil moisture via its control on the evaporation. However, the soil moisture via its control on the thermal inertia reduces the impact of the day-time evaporative cooling by reducing the nocturnal cooling. This newly identified moisture-related negative feedback can reduce the variability of the surface temperature in semiarid regions by up to a factor of 2. The model also provides a simple framework to understand the role of the thermal properties in the frequent cold bias identified in stratified stable atmospheric situations in the northern midlatitudes.

## 1. Introduction

The mean and the daily minimum and maximum values of the surface temperature are major indicators of the realism of the near-surface continental climate simulated by numerical models. These values are governed by the net surface radiation, by the turbulent fluxes, and by the heat conduction into the soil layers and their diurnal variations. Atmospheric process are generally thought to be the strongest (e.g., Comer & Best, 2012; Santanello et al., 2013). The impact of the land subsurface processes on the temperature in general is mainly attributed to the change of the surface energy budget via the soil moisture through its impact on the evaporation rate (e.g. Boé, 2013) and eventually on the precipitation with a positive (recycling) (Koster et al., 2003) or a negative effect (Taylor et al., 2012). The possible impact of the variations of heat conduction into the soil on the surface temperature is rarely discussed. Sensitivity experiments have shown that temperature biaises can be sensitive to the soil thermal properties. For instance, Sandu et al. (2013); Holtslag et al. (2013); and Sterk et al. (2013) found that a cold bias associated with stable boundary layer in numerical weather prediction simulations is reduced when increasing the skin layer thermal conductivity and Kumar et al. (2014) have shown that a warm bias impacting the simulated monsoon climate over South Asia is reduced when the prescribed soil heat capacity and heat conductivity are reduced. Wang et al. (2016) introduced a dependence of the soil thermal properties on moisture and texture in the land-surface module of a state-of-the-art climate model and found an impact on the short-term variability of the temperature at regional scale which can affect extreme events such as heat waves. Aït-Mesbah et al. (2015) discussed the role of thermal inertia in the large spread of the simulated surface temperature over arid and semiarid regions among climate models. They showed that the diurnal response of surface temperature to the thermal inertia is asymmetric between daytime and nighttime, inducing a change in the daily mean surface temperature that can reach several degrees over large areas in dry regions. However, none of these studies give a general framework highlighting the processes controlling the sensitivity of the mean temperature and of the diurnal temperature range to the thermal inertia.

This paper aims at clarifying the role of the soil thermal inertia variations induced by the soil moisture and the snow density in the surface temperature. A simplified model based on the surface energy budget is introduced in section 2. This model provides a framework to highlight the role of soil thermal inertia in the variation of the climatological mean value and mean diurnal amplitude of the surface temperature. The model's validity is verified in section 3 using global numerical simulations performed with the atmospheric and the land-surface modules of the Institute Pierre Simon Laplace Climate Model (IPSL-CM; Dufresne et al., 2013). The role of the thermal inertia and the atmospheric fluxes is discussed in section 4, and conclusions are presented in section 5.

## 2. A Simple Energy Budget-Based Model for Characterizing the Sensitivity of the Surface Temperature to the Thermal Inertia

The soil thermal volumetric heat capacity $C$ $(\mathrm{J.m^{-3}.K^{-1}})$ and the soil thermal heat conductivity $\lambda$ $(\mathrm{W.m^{-1}.K^{-1}})$ are crucial for the land subsurface thermal processes. They are soil moisture-dependent, i.e., increased soil moisture leads to higher soil thermal conductivity and capacity. These two parameters determine the thermal inertia, also called "heat effusivity" and is defined as $\Gamma=\sqrt{C\lambda}$ $(\mathrm{J.m^{-2}.K^{-1}.s^{-0.5}})$. The thermal inertia represents the resistance of soil to temperature change during a full-heating/cooling cycle. Hence, for a given temporal perturbation of the fluxes, the higher the thermal inertia, the lower the temporal change in surface temperature. Mean values over 24 h time period when the thermal conduction flux into the soil is positive (daytime) or negative (nighttime) are considered. The radiative fluxes are counted positive when they heat the surface, while the sensible, latent, and conduction fluxes are counted positive when they cool the surface. The diurnal amplitude $\Delta X$ of a particular variable is defined as the difference between its mean values during the day $X_d$ and during the night $X_n$. If the daily mean is $\overline{X}$, the day-time (resp. nighttime) half diurnal amplitude is $\Delta X_d = X_d - \overline{X}$ (resp., $\Delta X_n = \overline{X} - X_n$), and $\Delta X = \Delta X_d + \Delta X_n = X_d - X_n$. The diurnal amplitude is the sum of $\Delta X_d$ and $\Delta X_n$. The day-time and the nighttime mean temperature is defined as:

$$\begin{cases} T_{sd} = \overline{T_s} + \Delta T_{sd} \\ T_{sn} = \overline{T_s} - \Delta T_{sn} \end{cases} \tag{1}$$

Let $\alpha$ be the mean duration of the day. The mean temperature can be written as $\overline{T_s} = \alpha T_{sd} + (1-\alpha) T_{sn}$. When substituting $\overline{T_s}$ with its expression as a function of the day duration equation (1) can be rewritten as:

$$\begin{cases} \Delta T_{s_d} = (1-\alpha)\Delta T_s \\ \Delta T_{s_n} = \alpha \Delta T_s \end{cases} \tag{2}$$

The day-time and nighttime energy budget at the surface can be written as:

$$\begin{cases} R_d = F_d + G_d \\ R_n = F_n + G_n \end{cases} \tag{3}$$

where, $R$ is the net radiation flux at the surface, $G$ is the thermal heat flux into the soil, and F is the turbulent heat flux at the surface.

The diurnal amplitude reads

$$\Delta R = \Delta F + \Delta G \tag{4}$$

The half-diurnal amplitude of the turbulent fluxes is assumed to depend linearly on the half diurnal amplitude of the temperature $T$.

$$\begin{cases} \Delta F_d = F'_d . \Delta T_{s_d} \\ \Delta F_n = F'_n . \Delta T_{s_n} \end{cases} \tag{5}$$

where $F'$ is the sensitivity of the turbulent fluxes to the surface temperature.

Adding the two equations in (5) and using (2), the diurnal amplitude for the turbulent fluxes can be rewritten:

$$\Delta F = [(1-\alpha)F'_d + \alpha F'_n]\Delta T_s \tag{6}$$

For an idealized diurnal cycle of $T_s$ sinusoidal in time, the diurnal amplitude of G, can be written as a function of that of the diurnal amplitude of Ts

$$\Delta G = \Gamma\sqrt{\frac{2\pi}{\tau}}\Delta T_s \tag{7}$$

where $\tau$ is equal to the duration of the day (24 h) (Wang et al., 2010) and the diurnal amplitude is taken as the difference between the maximum and the minimum values for G and $T_s$. Figure 1 shows that the diurnal cycle of the temperature is close to a sinusoid. We verified that equation (7) performs similarly well when the diurnal amplitude is defined according to the maximum and minimum values or according to the positive and negative anomalies with respect to the mean value (as done in this paper).

Substituting equations (6) and (7) in (4) leads to

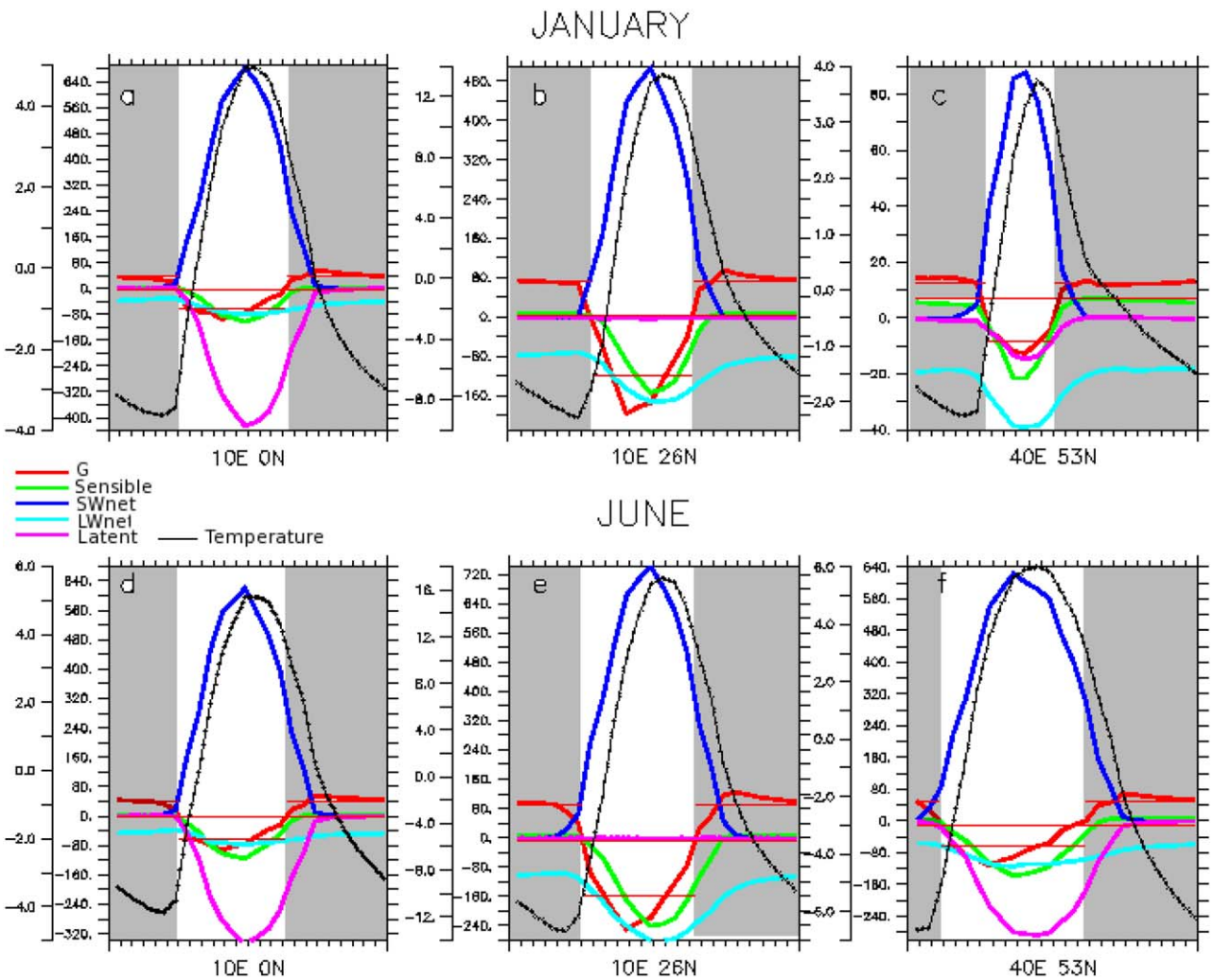


**Figure 1.** Climatological diurnal cycle of the surface temperature (black line left most vertical scale (degree Celsius)) and of the surface energy budget terms: Sensible heat flux (green), net shortwave radiation at the surface (dark-blue), net longwave radiation at the surface (light blue), latent heat flux (pink), heat conduction into the soil, G (red) (in W.m$^{-1}$). The horizontal lines show the day-time, the nighttime (see definitions in the text) and the daily mean climatological values of G. Results are displayed for specific points in space representing (left column: a and d) moist tropical regions, (middle column: b and e) desert, and (right column: c and f) boreal for (top row) January and (bottom row) June. The light grey background indicates the nighttime period.

$$\Delta T_s = \frac{\Delta R}{\Gamma\sqrt{\frac{2\pi}{\tau}} + [(1-\alpha)F'_d + \alpha F'_n]} \tag{8}$$

Which allows for the estimation of the sensitivity of the diurnal amplitude of the temperature to the thermal inertia.

$$\frac{\partial \Delta T_s}{\partial \Gamma} = -\frac{\sqrt{\frac{2\pi}{\tau}}\Delta R}{\left(\Gamma\sqrt{\frac{2\pi}{\tau}} + [(1-\alpha)F'_d + \alpha F'_n]\right)^2} + \frac{\partial \Delta R}{\partial \Gamma}\frac{1}{(\Gamma\sqrt{\frac{2\pi}{\tau}} + [(1-\alpha)F'_d + \alpha F'_n])} \tag{9}$$

The first term in equation (9) is the sensitivity of $\Delta T_s$ to $\Gamma$ when $\Delta R$ is independent of $\Gamma$, $\frac{\partial \Delta T_s}{\partial \Gamma}|_{\Delta R=cst}$, and the second term is the contribution due to the sensitivity of $\Delta R$ to $\Gamma$, $S_{R,\Gamma}$. Numerical simulations show that $S_{R,\Gamma}$ is less than 20% of the absolute value of $\frac{\partial \Delta T_s}{\partial \Gamma}|_{\Delta R=cst}$ and that it exhibits similar geographical patterns (see Appendix A for more details). This supports the hypothesis that the sensitivity of $\Delta T_s$ to $\Gamma$ is correctly represented by $\frac{\partial \Delta T_s}{\partial \Gamma}|_{\Delta R=cst}$. In the rest of the paper, the sensitivity of $\Delta R$ to $\Gamma$ is neglected and $S_{R,\Gamma}$ is set equal to 0.

We now focus on the mean surface temperature. Let $F_{d_0}$ and $F_{n_0}$ be the day-time and nighttime turbulent fluxes corresponding to a reference temperature $T_{s_0}$. The day (resp. the night) is defined as the period when the temperature anomaly (with respect to the mean daily temperature) is positive (resp. negative).

$$\begin{cases} F_d = F_{d_0} + F'_d.(T_{sd} - T_{s_0}) \\ F_n = F_{n_0} + F'_n.(T_{sn} - T_{s_0}) \end{cases} \tag{10}$$

At equilibrium, the sum of the day-time and nighttime thermal heat fluxes into the soil is close to zero.

$$\alpha G_d + (1-\alpha)G_n \approx 0 \tag{11}$$

Equation (11) is verified close to the equator. Apart from equator, it is an approximation which corresponds to an idealized situation where no seasonal variations of the mean surface temperature occur throughout the month. The seasonal variation of the mean temperature induces a slight departure of the closure of the mean daily energy budget of the order of 5 to 15 W m$^{-2}$. It can reach locally 20 W m$^{-2}$ in regions where snow melting is likely to occur.

Combining equations (3),(10), and (11),

$$\alpha R_d + (1-\alpha)R_n \approx \alpha F_{d0} + (1-\alpha)F_{n0} + \alpha F'_d(T_{sd} - T_{s_0}) + (1-\alpha)F'_n.(T_{sn} - T_{s_0}) \tag{12}$$

For an infinite thermal inertia, the diurnal amplitude of the surface temperature is equal to zero and the mean value $T_{s_0}$, the daytime $T_{sd}$ and the nighttime $T_{sn}$ values are identical. Assuming that the net radiation is independent of the thermal inertia (as discussed in the appendix, it is a reasonable assumption at the first-order), the right-hand side member of (12) is independent of $\Gamma$. This makes possible to rewrite equation (12) as:

$$\alpha R_d + (1-\alpha)R_n \approx \alpha F_{d0} + (1-\alpha)F_{n0} \tag{13}$$

and

$$\alpha F'_d(T_{sd} - T_{s_0}) + (1-\alpha)F'_n.(T_{sn} - T_{s_0}) \approx 0 \tag{14}$$

Setting $\overline{F'} = \alpha F'_d + (1-\alpha)F'_n$, the temperature $T_{s_0}$ can be written as follows:

$$T_{s_0} \approx \frac{\alpha F'_d T_d + (1-\alpha)F'_n T_n}{\alpha F'_d + (1-\alpha)F'_n} \tag{15}$$

Using equations ((2), (5), and (6)), one can derive the expression for $\overline{T_s}$.

$$\overline{T_s} = T_{s_0} - \alpha(1-\alpha)\frac{F'_d - F'_n}{\overline{F'}}\Delta T_s \tag{16}$$

Since $T_{s_0}$ is independent of the thermal inertia, the expression of the sensitivity of the mean daily surface temperature to the thermal inertia can be deduced as follows:

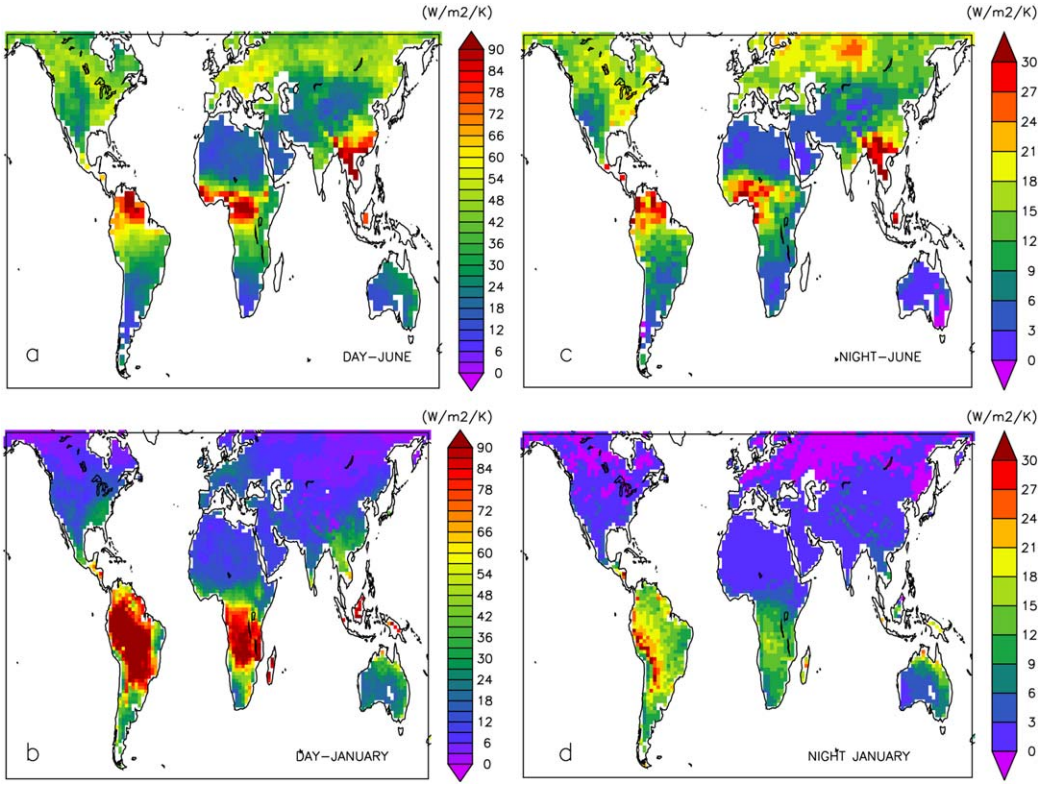


**Figure 2.** Climatological sensitivity of the sum of the latent and sensible heat fluxes to the surface temperature (in $W.m^{-2}.K^{-1}$): (a) during daytime in June, (b) during daytime in January, (c) during nighttime in June, and (d) during nighttime in January.

$$\frac{\partial \overline{T_s}}{\partial \Gamma} = \alpha(1-\alpha)\frac{F'_d - F'_n}{\overline{F'}}\frac{\sqrt{\frac{2\pi}{\tau}}\Delta R}{\left(\Gamma\sqrt{\frac{2\pi}{\tau}} + [(1-\alpha)F\prime_d + \alpha F\prime_n]\right)^2} \tag{17}$$

The sensitivity of the mean surface temperature to the thermal inertia (given by equation (17)) is equal to the sensitivity of the diurnal amplitude of the surface temperature (given by equation (9)) weighted by a factor $\alpha(1-\alpha)\frac{F'_d - F'_n}{\overline{F'}}$. This factor depends on the duration of the day and on the contrast between the daytime and the nighttime sensitivity of the turbulent fluxes to the surface temperature. It is always smaller than 1 (since $F'_d$ and $F'_n$ are always positive and $F'_d > F'_n$, see Figure 2). Analyzing the ratio $\frac{\delta T_n}{\delta T_d}$, Aït-Mesbah et al. (2015) highlighted the diurnal contrast of the stability state of the boundary layer responsible of the asymmetrical response of the surface temperature to the thermal inertia leading to the sensitivity of the mean temperature to the thermal inertia. The conceptual model presented here allows to quantitatively evaluate the impact of the turbulent fluxes on the sensitivity of the mean temperature and the diurnal amplitude to the thermal inertia.

## 3. Evaluation of the Simplified Model With 3-D Numerical Simulations

### 3.1. The Coupled LSM-Atmospheric Model

LMDZOR is the atmosphere-land component of the IPSL-CM (Dufresne et al., 2013). LMDZ is the atmospheric General Circulation Model (GCM) that has been developed for about 30 years at the Laboratoire de Météorologie Dynamique. The model resolution for this study is 3.75° (latitude) by 1.85° (longitude) with 39 vertical levels. The physical parameterizations implemented in the LMDZ5B version used here are described in Hourdin et al. (2013), Rio and Hourdin (2008a), and Rio et al. (2013). In the boundary layer, a combination of the thermal plume model (Rio & Hourdin, 2008b) for the representation of the organized structures of the convective boundary layer and a small-scale turbulence scheme (Yamada, 1983) is used. This small-scale

turbulence scheme based on the evolution of the turbulent kinetic energy, which is parameterized as a function of mixing length and a velocity which characterize the turbulent displacements. A minimum mixing length is prescribed to 1 m, which corresponds to situations where no mixing occur and the surface is decoupled from the atmosphere. The surface boundary layer is treated according to Louis (1979). The formulation of the stability functions is based on the Richardson number and depends on the degree of stability of the atmosphere. The drag coefficients are computed with prescribed roughness lengths provided by the Land Surface Model.

The Land Surface is the ORCHIDEE model (Krinner et al., 2005). The roughness lenghts are prescribed as a function of the land-cover type (bare soil, vegetation, ice) and height (prescribed for each Plant Functional Type -PFT-) and are identical for the momentum and for the heat transfer. The parameterization of the soil hydrology allows for a physically based description of vertical water fluxes, using Richards equation (De Rosnay et al., 2002; d'Orgeval et al., 2008). For the heat diffusion into the soil ORCHIDEE resolves a diffusion equation for heat based on a Fourier Law with a zero flux condition at a limited soil depth. A common vertical discretization is adopted for heat and moisture transfer up to 10 m total depth and the soil thermal properties are parameterized as a function of the soil moisture and the soil texture (Wang et al., 2016). The snow thermal properties are parameterized as a function of the snow density. The water and energy budgets are computed at the same time step as the atmospheric physics. The surface temperature is computed using an implicit scheme coupling the atmosphere and the land-surface.

### 3.2. The Numerical Experiment

When constructing sensitivity experiments with a given climate model a challenge is to isolate the effects of the modified parameter from the model internal variability, especially when the effects are weak. The traditional way of addressing this issue is to run paired experiments (with and without modification) under unconstrained meteorology over decades or hundreds of years (Forster & Taylor, 2006). This approach requires long computing time to simulate the full range of climate variability (Kooperman et al., 2012). A way to reduce the internal variability is to constrain the large-scale atmosphere dynamics toward prescribed atmospheric conditions using a nudging approach (Coindreau et al., 2007). This method has been successfully used to evaluate the parameterizations related to the land-surface/atmosphere coupling (Cheruy et al., 2013). The simulated global wind fields (zonal u; meridional v) are nudged with the ECMWF reanalyzed winds by adding a linear restoring term with a 6 h relaxing time ($\tau_{nudge}$). Here 6 year long runs over the period 1990–1995 have been performed with the LMDZOR model following the Atmospheric Model Intercomparison Project (AMIP) protocol where the AGCM is constrained by realistic sea surface temperature and sea ice. The model outputs are archived with an hourly frequency and a mean monthly diurnal cycle is reconstructed. The soil thermal inertia of the Earth surface ranges from 800 $(J.m^{-2}.K^{-1}.s^{-0.5})$ to 2,500 $(J.m^{-2}.K^{-1}.s^{-0.5})$ while the snow thermal inertia ranges from 200 $(J.m^{-2}.K^{-1}.s^{-0.5})$ for fresh snow to 600 $(J.m^{-2}.K^{-1}.s^{-0.5})$ for compact snow. We run several sensitivity experiments using the numerical model with thermal properties that can either vary as a function of the soil moisture and age of the snow or can be uniformly prescribed independently of the soil moisture and the age of the snow. In the latter case, we run three simulations with low, medium, and high thermal inertia values being applied to both the soil and the snow simulataneously. The thermal inertia is set to 850, 1,680, and 2,400 $(J.m^{-2}.K^{-1}.s^{-0.5})$, respectively, equivalent to the dry, intermediate, and moist soil conditions and the snow thermal inertia to 100, 350, and 500 $(J.m^{-2}.K^{-1}.s^{-0.5})$, respectively, equivalent to fresh, intermediate, and old snow conditions. The various sensitivity experiments are summarized in Table 1. Note that in these experiments, only the interaction between the thermal inertia and the soil moisture is switched off, the interactions between rainfall, soil moisture, and evaporation are maintained.

**Table 1**
*Values of the Thermal Inertia Used in the Sensitivity Experiment Run With LMDZOR*

| Experiment | $\Gamma$ soil $(J.m^{-2}.K^{-1}.s^{-0.5})$ | $\Gamma$ snow $(J.m^{-2}.K^{-1}.s^{-0.5})$ |
|---|---|---|
| $\Gamma_{low}$ | 850 | 100 |
| $\Gamma_{inter}$ | 1,680 | 350 |
| $\Gamma_{high}$ | 2,400 | 500 |
| $\Gamma_{var}$ | Function of soil moisture | Function of the density of snow |

A climatological monthly mean diurnal cycle is constructed by averaging the 180 single values of the temperature and the energy budget components for each individual hour of the 24 h period. Figure 1 shows the mean diurnal cycle of the various components of the surface energy budget and the surface temperature anomaly for a moist tropical regions (10E'0°N), a desert area (10E'28°N), and a midlatitude continental area (100E'57°N) in January and June. A phase-shift between the temperature and the various terms of the energy budget is visible on the plots. During the night the energy budget mostly

results from the infrared cooling and the thermal conduction warming by the soil. At high latitudes, especially in winter and during the night, the sensible heat flux contributes to the warming of the surface as the atmosphere is warmer than the soil surface (see Figure 1f). During the day, the relative contribution of the different terms of the energy budget varies strongly according to the regions and the season. In tropical areas (see Figures 1a and 1d), the turbulent fluxes (especially the latent heat flux) contribute the most to the cooling of the surface and the heat conduction is negligible. Over the deserts (Figures 1b and 1e), the sensible heat flux, the heat conduction, and the LW radiation respond with similar intensities to the solar warming. For mid/high-latitudes areas in summer (see Figure 1c), the contributions are comparable to the ones of the tropical areas, with a strong day/night duration asymmetry at the highest latitudes. In winter, the latent heat plays a minor role, while the LW cooling contributes the most to the cooling of the surface.

The horizontal red lines on Figure 1 depict the nighttime and the day-time values of G used in the simplified model as well as the daily mean value of G. The day duration $\alpha$ is estimated as the fraction of the day when the soil gains energy, i.e., when the climatological mean diurnal anomaly of G is positive. Note that the definition is not identical to the classical definition referring to the availability of shortwave radiation. The evaluation of $\alpha$ from a climatological monthly mean diurnal cycle can be an issue especially at high latitudes where the day-duration can vary significantly during a month. The budget is nearly closed as demonstrated by the near zero value of G over a 24 h period for each region. The small departures from the closure are due to the seasonal variation of the mean surface temperature which is not rigorously at equilibrium apart from equator. The departure is of the order of 5–15 W.m$^{-2}$ and can reach 20 W.m$^{-2}$ when snow melting is likely to occur.

The sensitivity parameters $F'_d$ and $F'_n$ are estimated as the slope of the linear regression between the climatological hourly estimations of the sum of the turbulent latent and sensible heat flux and the surface temperature. The period of positive $(T_s - \overline{T_s} > 0)$ anomaly of the temperature is used to estimate the day-time

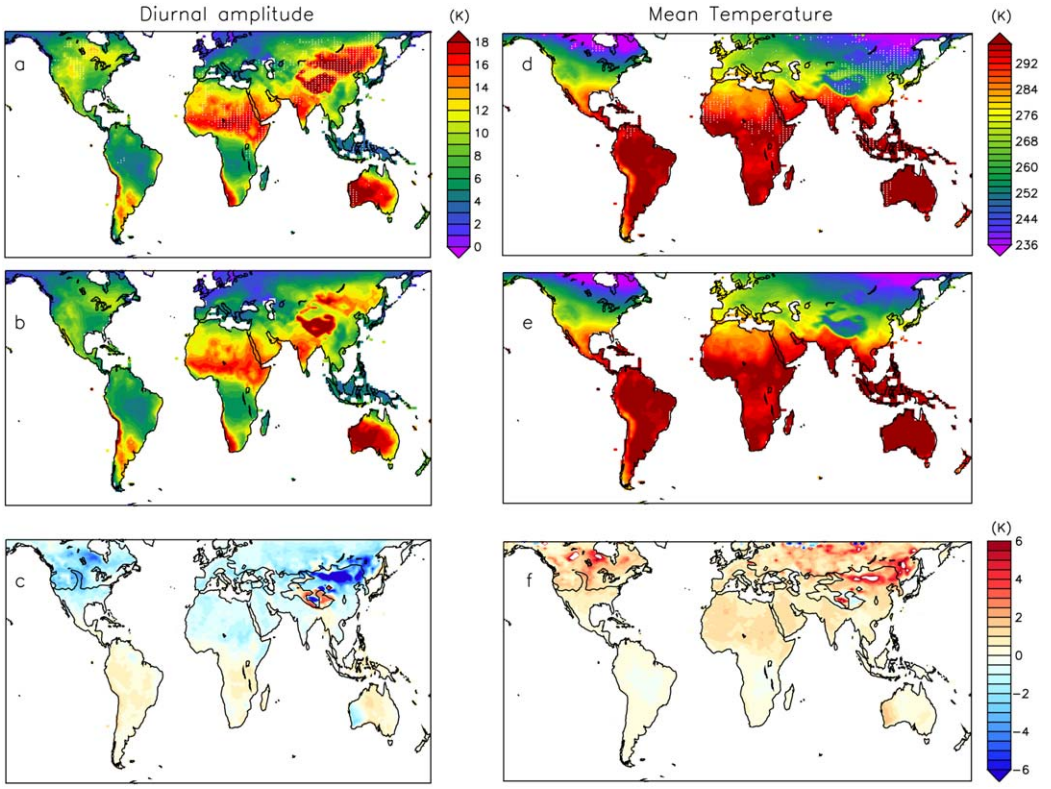


**Figure 3.** Climatological diurnal amplitude of (left column) surface temperature and (right column) daily mean surface temperature in January computed using the (top row) conceptual model and (middle row) estimated using LMDZOR. The difference (conceptual – LMDZOR) is shown on the bottom row. Units are *K*. The white-shaded areas correspond to regions where the differences are significant at 99% with a *t* test.

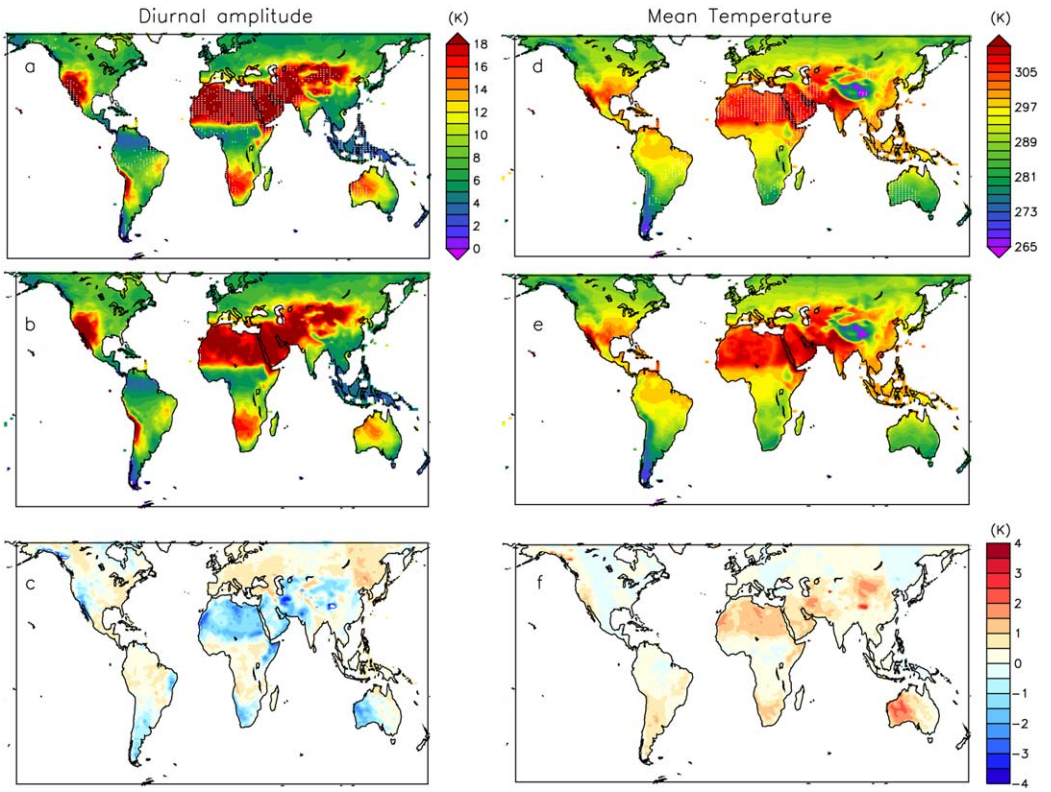


**Figure 4.** Climatological diurnal amplitude of (left column) surface temperature and (right column) daily mean surface temperature in June computed using the (top row) conceptual model and (middle row) estimated using LMDZOR. The difference (conceptual – LMDZOR) is shown on the bottom row. Units are *K*. The white-shaded areas correspond to regions where the differences are significant at 99% with a *t* test.

sensitivity parameters $F'_d$ and the period of negative anomaly $(T_s - \overline{T_s} < 0)$ is used to estimate the nighttime sensitivity parameter $F'_n$. To evaluate the sensitivity parameters, we use the temperature instead of the heat conduction flux anomalies because of the phase shift between diurnal cycle of the surface temperature and G mentioned above. The maps of $F'_d$ and $F'_n$ are displayed on Figure 2. The patterns are strongly modulated by the season. The sensitivity of the turbulent fluxes to the surface temperature is strong over moist areas, and low over deserts. For a given season, the patterns are similar for day-time and nighttime. As expected, the sensitivity of the turbulent fluxes to the surface temperature is stronger during the day and in convective regions where the boundary layer is unstable. The sensitivity is weaker during the night and in winter when stable boundary layers are likely to occur. In this case, the turbulent fluxes become small compared to the (predominately LW) radiative fluxes, which dominate the surface energy budget (see Figure 1f for instance).

The mean diurnal amplitude and the mean daily value of the surface temperature are estimated from equations (8) and (16) of the conceptual model, neglecting the sensitivity of $R$ to $\Gamma$. They are compared to the same quantities estimated with the full LMDZOR model for the climatological months of January (Figure 3) and June (Figure 4). The degree of significance of the difference has been evaluated with a Student *t* test. The regions where the differences between the conceptual model and LMDZOR are significant at 99% are shaded in white. Overall, the structures of the mean daily temperature and mean diurnal amplitude of the surface temperature are correctly reproduced by the conceptual model and the differences are generally not statistically significant. Over the desert and especially the Sahara, the conceptual model significantly overestimate the diurnal amplitude. This can be due to the omission of $\frac{\partial R}{\partial \Gamma}$. In winter, the diurnal amplitude is significantly overestimated by the conceptual model in a region located close to the border of snow covered areas in the Southern part of the Siberia (the 10% mean snow fraction is indicated by a black line on Figure 3c). Here, it is possible that the snow melting plays a role in areas partially covered by snow but the

conceptual model does not account for it. For the northern part of the region, it is also possible that equation (11) is less valid as mentioned in the section 2.

## 4. Roles of Thermal Inertia in the Surface Temperature

The estimation of the mean surface temperature and of the climatological diurnal amplitude of the surface temperature done with the conceptual model are consistent with the diagnostics from LMDZOR integrations. The conceptual model can now be used to investigate the response of the mean and the diurnal amplitude of the temperature to the various components of the surface energy budget and to the thermal inertia.

### 4.1. Mean Diurnal Amplitude of the Temperature and Surface Energy Budget

The following discussion mainly relies on the analysis of the various terms of equation (8) of the conceptual model. When the turbulent fluxes are independent of the temperature (i.e., $F'_d$ and $F'_n$ equal to 0 in equation 8), the diurnal amplitude of the surface temperature can reach very high values (Figures 5b and 5f). As it can be expected from equation (8), the spatial structure of the diurnal amplitude of the temperature is similar to the one of the diurnal amplitude of the net radiation at the surface (Figures 5a and 5e) with the exception of the borders of snow-covered areas where the diurnal cycle is overestimated by the model as previously noted. When the full equation (8) is considered (i.e., $F'_d$ and $F'_n$ not equal to 0 in equation 8), the spatial structure of the diurnal amplitude of the temperature (Figures 5d and 5h) is significantly modified and strongly reduced over moist areas such as Amazonia, Central Africa, Maritime continent, and the South Eastern Asia in boreal summer, which correspond to areas where the sensitivity of the sum of sensible and latent heat fluxes to the surface temperature weighted by the duration of the day and the night ($(1-\alpha)F'_d+\alpha F'_n$) is high

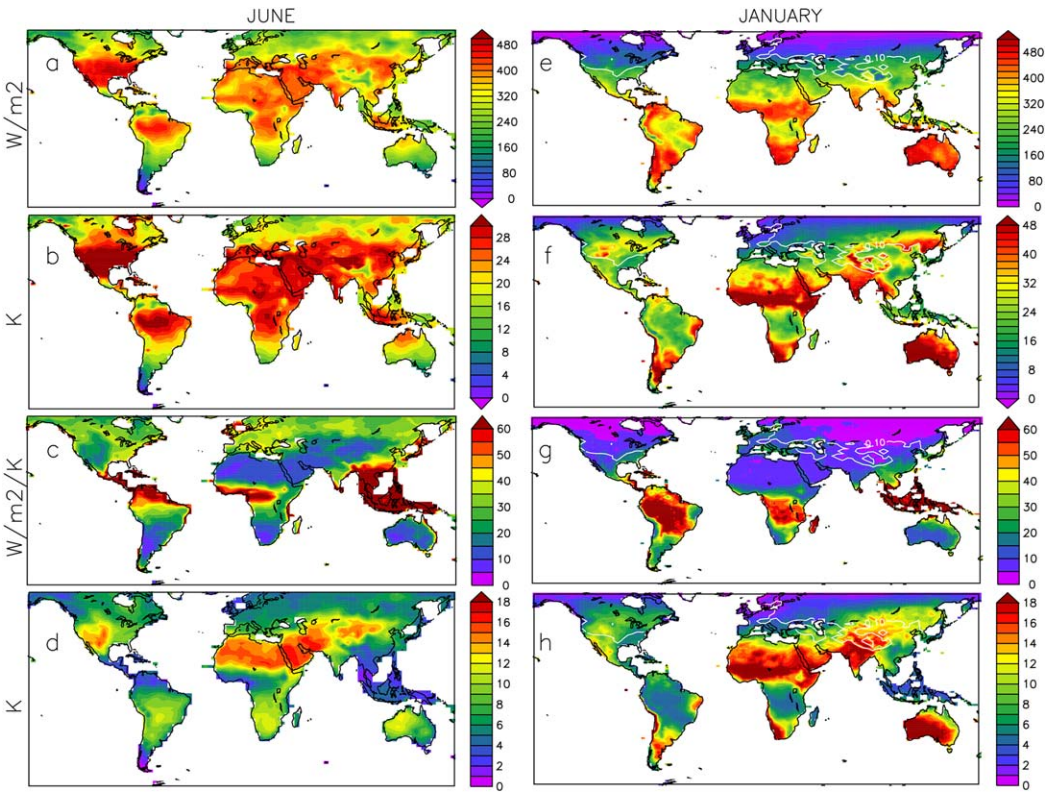


**Figure 5.** Main terms composing the mean sensitivity of the diurnal amplitude to the thermal inertia for a climatological month of (left column) JUNE and (right column) JANUARY. (a, e) Diurnal amplitude of the net radiation at the surface. (b, f) Diurnal amplitude of the surface temperature when the turbulent fluxes are independent of the temperature. (c, g) Mean sensitivity of the sum of the sensible and latent heat fluxes to the surface temperature weighted by the duration of day and the night. (d, h) Climatological diurnal amplitude ($T_{sd}-T_{sn}$) of the surface temperature. The white line on the January plots depicts the 10% mean snow fraction level.

(Figures 5c and 5g). Conversely, the diurnal amplitude is large over Southern Siberia in boreal winter, where the sensitivity of the turbulent fluxes to the surface temperature is minimum and is of about the same order as that of the thermal inertia term in equation (8).

Assuming that the sensitivity of the turbulent fluxes to the surface temperature is proportional to the fluxes (to the first-order), the stronger the contribution of the turbulent fluxes to the surface energy budget, the smaller the sensitivity of the diurnal amplitude of the surface temperature to the thermal inertia.

### 4.2. Impact of the Thermal Inertia on the Mean Daily Temperature

The climatological sensitivity of the surface temperature to the soil thermal inertia is quantitatively evaluated. On the one hand, we compute $\frac{\partial \overline{T_s}}{\partial \Gamma}$ (respectively $\frac{\partial \Delta T_s}{\partial \Gamma}$) with the equation (17) (resp. (9)) of the conceptual model whose parameters are evaluated with the integration $\Gamma_{inter}$ of LMDZOR. One the other hand we use two integrations of LMDZOR, $\Gamma_{high}$ and $\Gamma_{low}$ summarized in Table 1 to evaluate numerically the variation of mean temperature and of diurnal amplitude associated with the variation of thermal inertia between high and low values.

The maps of $\frac{\partial \overline{T_s}}{\partial \Gamma}\Delta\Gamma$ and $\frac{\partial \Delta T_s}{\partial \Gamma}\Delta\Gamma$ for the month of June and January are shown in Figure 6. $\Delta\Gamma$ is the difference of the prescribed thermal inertia.

The results using the conceptual model and using the numerical integration of LMDZOR are in good agreement especially for the diurnal amplitude, although the results of the conceptual model are slightly noisier over the northern hemisphere in winter. As expected from equations (8) and (17), the regions where the diurnal amplitude and the daily mean values of the surface temperature are the most sensitive to the thermal inertia are the same.

When the sensitivities of the turbulent fluxes to the surface temperature, $F'_d$ and $F'_n$, are low, the sensitivity to thermal inertia is high because the thermal inertia term $(\Gamma\sqrt{\frac{2\pi}{\tau}})$ dominates in the denominator of

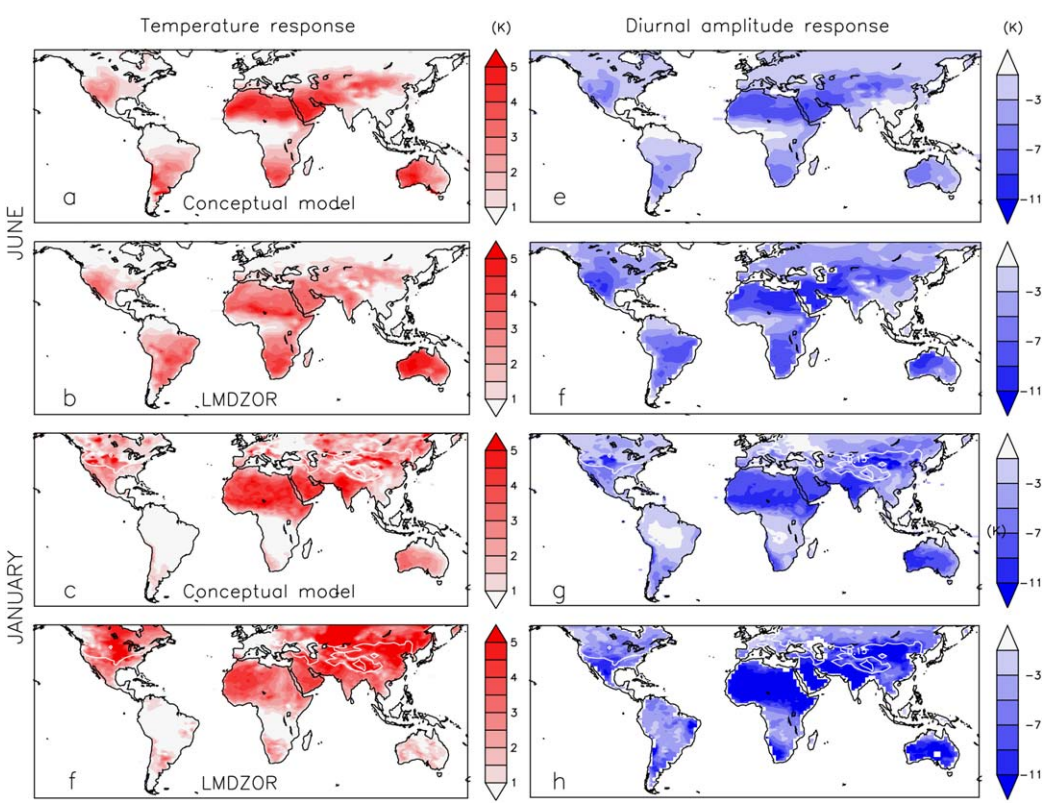


**Figure 6.** Response of the (left column) mean surface temperature and of the diurnal amplitude of the (right column) surface temperature to a change of the soil thermal inertia from 2,400 to 850 ($(J.m^{-2}.K^{-1}.s^{-0.5})$ for the soil and from 500 to 200 $[J.m^{-2}.K^{-1}.s^{-0.5})$ for the snow. The responses are computed in June for the (a, e) conceptual model and for the (b, f) reference model and in January for the (c, g) conceptual model and for the (f, h) reference model. Units are K.

equations (9) and (17). In January over a large part of the northern mid and boreal latitudes and during the whole year over arid and semiarid regions, the sensitivity of the turbulent fluxes to the surface temperature is low (Figures 5c and 5d) inducing a high sensitivity of the diurnal amplitude of the surface temperature (up to 10K) (Figures 6e and 6g) and a high sensitivity of the surface temperature to the soil thermal inertia (up to 5K, Figures 6a and 6c).

The conceptual model shows that the sensitivity of the surface temperature to the thermal inertia is controlled by both the soil thermal inertia and the turbulent fluxes. This conceptual model provides a framework to explain why several authors found that a persistent cold bias in stratified stable atmospheric situations is sensitive to the soil thermal properties (Holtslag et al., 2013; Sandu et al., 2013). If the cold bias is due to an underestimation of the soil thermal inertia, artificially enhancing the turbulent diffusion will lead to an increase in the turbulent fluxes and to a reduction of the sensitivity to the thermal inertia and will in turn lead to a reduction of the bias. On the other hand an increase in soil thermal inertia leads to an inhibition of the surface cooling and an increase of the daily mean surface temperature.

### 4.3. Role of the Soil Moisture Dependence of the Thermal Inertia on the Day-to-Day Variability of the Surface Temperature

The conceptual model shows that thermal inertia is a potential source of variability for the surface temperature through the amplitude of the diurnal cycle of the surface temperature. Over vegetated areas and bare soils, the soil moisture is the main source of variation for the soil thermal properties at daily time scale. In section 4.2, we demonstrated that the mean temperature increases and the diurnal amplitude decreases when the soil thermal inertia increases. Aït-Mesbah et al. (2015) showed that in arid and semiarid regions the diurnal response of surface temperature to the thermal inertia is asymmetric between daytime and nighttime and that the nighttime temperature is more sensible to the soil thermal inertia. An increase of

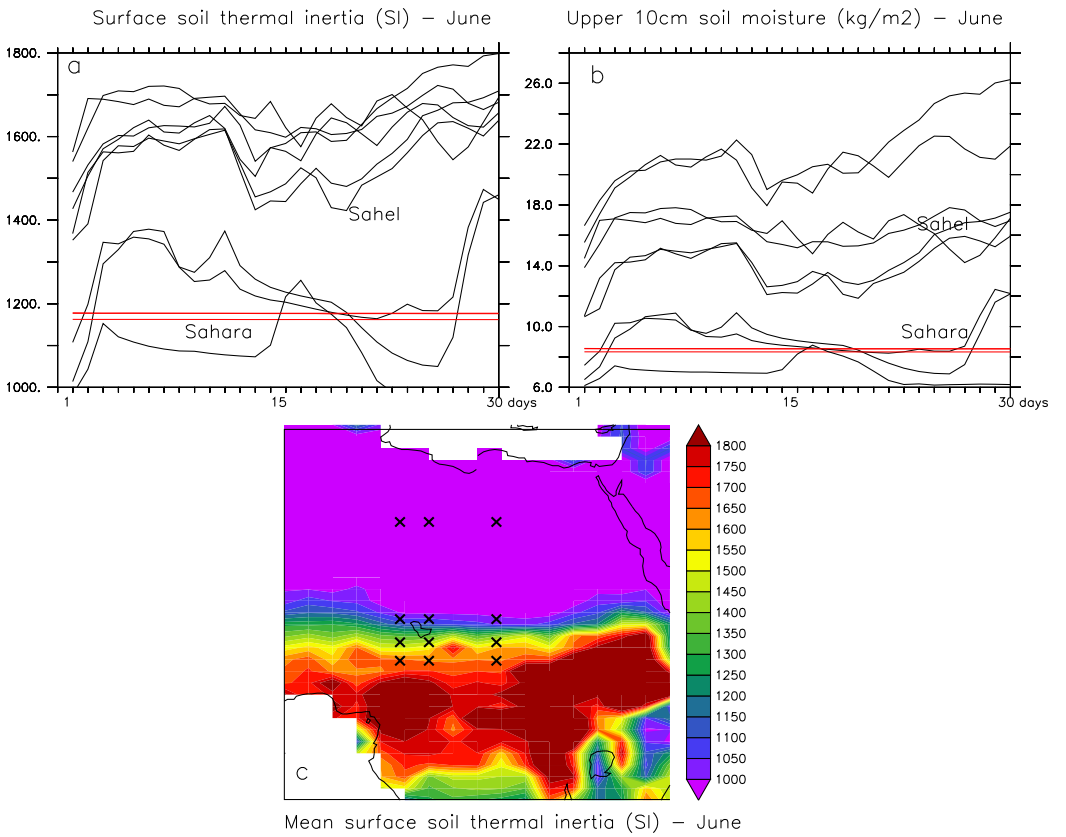


**Figure 7.** Day-to-day variations of the (a) thermal inertia and of the (b) moisture in the upper 10 cm of soil, (c) mean soil thermal inertia in June. The black points in Figure 7c represents the grid points for which the variations of the thermal inertia and of the soil moisture are plotted in Figures 7a and 7b. The red lines are for the points located over Sahara while the black line are used for the points located in semiarid area.

soil thermal inertia as it occurs when the soil moistens induces an increase of nocturnal temperature. In semiarid regions, the soil is mostly dry and moistens during the convective events. This introduces a day-to-day variability of the thermal inertia which is well phased with the soil moisture in the upper soil layer (Figure 7). The contribution of the variability (represented by the variance) of the thermal inertia through soil moisture variations to the variability (represented by the variance) of the surface temperature at the diurnal time scale is evaluated with the following index

$$V_{\Gamma,moist} = \frac{\sigma^2(T)_{\Gamma_{var}} - \sigma^2(T)_{\Gamma_{fixed}}}{\sigma^2(T)_{\Gamma_{var}}} \tag{18}$$

where $\Gamma_{var}$ refers to the control run performed with LMDZOR and with the thermal inertia depending on the soil moisture and $\Gamma_{inter}$ refers to the sensitivity experiment performed with LMDZOR and a prescribed value of the thermal inertia set to an intermediate value of (1,680 $J.m^{-2}.K^{-1}.s^{-0.5}$) which is independent of the soil moisture content. This approach has been used by several authors (see Seneviratne et al., 2010 for a review) to diagnose the sensitivity of climate processes to the land conditions at interannual or intra-annual time scale. Figure 8 shows $V_{\Gamma,moist}$ evaluated for the months of JJA with LMDZOR for the daily mean, daily minimum, and daily maximum temperature. The variability of the thermal inertia with the soil moisture reduces the variability of the surface temperature over regions such as Sahel and India by 20–50%. In these regions, monsoons induce a high day-to-day variability of the thermal inertia which induces a high day-to-day variability of the daily minimum of temperature when the soil heat transfer is a significant component of the surface energy budget. These regions lie in the transition zones between wet and dry climates. In these regions, positive anomalies of the soil-moisture induce negative anomalies of the near surface temperature, through an increased evaporative cooling. The results presented here highlight a negative feedback loop: positive anomalies of the soil moisture lead to an increase of the soil thermal inertia and to a reduction of the nocturnal cooling. This latter process reduces the well-known day-time cooling impact of

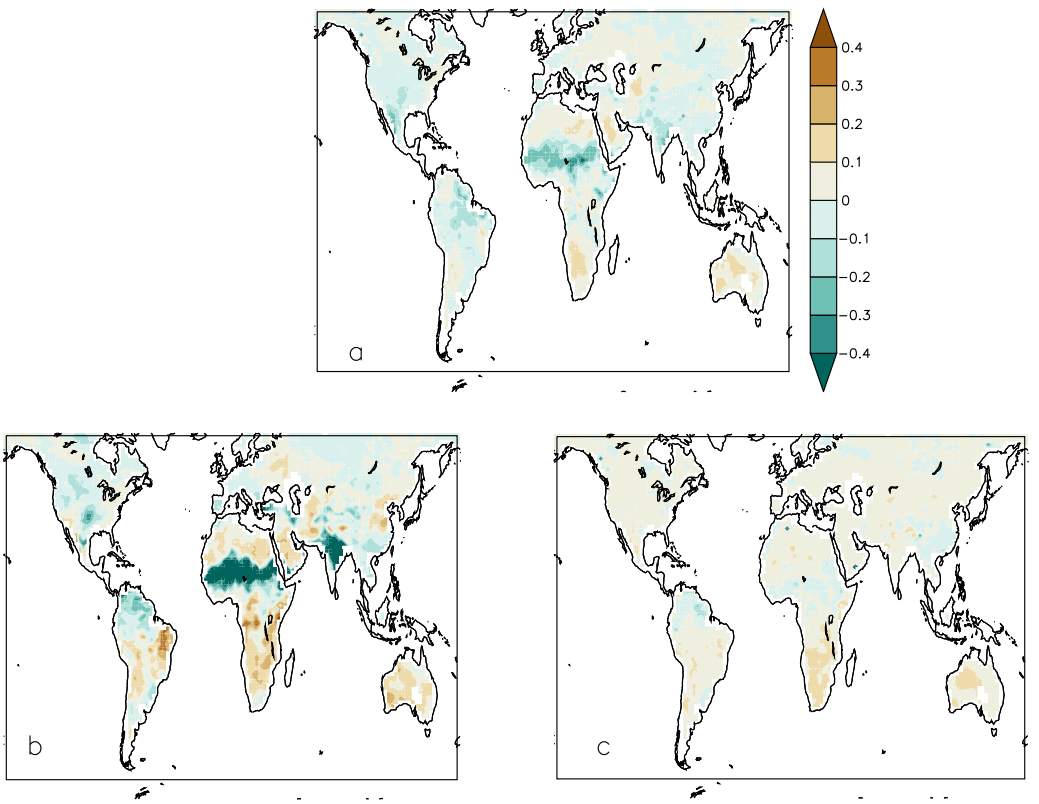


**Figure 8.** Contribution of the day-to-day variability of the thermal inertia to the day-to-day variability of the surface temperature ($V_{\Gamma,moist}$, see text) in JJA: (a) $V_{\Gamma,moist}$ is plotted for the mean surface temperature, (b) $V_{\Gamma,moist}$ is plotted for the minimum surface temperature, and (c) $V_{\Gamma,moist}$ is plotted for the daily maximum surface temperature. No units.

the soil moisture mentioned previously. This result is consistent with the results of Kumar et al. (2014) showing a reduced warm bias during the monsoon season due to a decrease in the prescribed thermal inertia from values typical of moist conditions to values closer to dry conditions consistently with the semiarid characteristics of the region.

## 5. Conclusions

The sensitivity of the mean climatological diurnal amplitude of the surface temperature and that of the daily mean surface temperature to the soil thermal inertia were expressed as a function of the mean sensitivity of the turbulent fluxes to the surface temperature, the diurnal amplitude of the net radiation at the surface, the thermal inertia itself, and the duration of the day using a conceptual model based on the surface energy budget. Three-dimensional numerical simulations performed with the atmospheric (LMDZ) and land surface (ORCHIDEE) modules of the IPSL climate model support the relevance of the conceptual model. The overall impact of an increase of soil thermal inertia is an increase of the mean climatological surface temperature and a decrease of the mean diurnal amplitude of the surface temperature.

In moist regions, the diurnal amplitude of the surface temperature and the daily mean surface temperature are controlled by the latent heat flux and the role of the thermal inertia is negligible. In regions where evaporation is limited, the sensitivity of the surface temperature to the thermal inertia is increased provided that the sensitivity of the turbulent fluxes to the surface temperature is small enough, i.e., is of the same order of magnitude or less than $\Gamma\sqrt{\frac{2\pi}{\tau}}$) and the contrast between the day and night turbulent fluxes is high.

In boreal winter, latent heat flux is negligible and sensible heat flux is weak. In such cases, the mean surface temperature is shown to be sensitive to the thermal inertia and the intensity of the sensitivity is controlled by both the thermal inertia and the sensitivity of the sensible heat flux to the surface temperature. The intensity of the sensitivity can be reduced either by increasing the thermal inertia or by increasing the turbulence, both leading to a surface warming. The sensitivity of surface temperature cold bias to the soil thermal inertia and the vertical diffusion found by several authors in numerical simulations of stratified stable atmospheric situations is explained by this conceptual model.

In the regions where the latent heat flux exhibits a high day-to-day variability, such as semiarid regions, the sensitivity of the surface temperature to the thermal inertia is increased. In these not too wet (energy limited) and not too dry (moisture limited) soil moisture (SM) hot spots, it is generally admitted that the variability of the surface temperature is explained by the soil moisture through its control on the evaporation. This work highlights a new moisture related negative feedback. This negative feedback can reduce the variability of the day-to-day surface temperature by up to a factor of two in semiarid regions where the high-frequency variability is generally explained by the control of the soil moisture on the day-time evaporation.

Overall, to correctly account for the soil-moisture temperature feedback and also remove some surface temperature biases in climate simulations, the thermal properties must be parameterized as a function of the soil moisture and the snow density which in turn have to be correctly simulated at the diurnal time-scale.

## Appendix A: A Evaluation of the Sensitivity of the Diurnal Amplitude of the Net Radiation to the Soil Thermal Inertia

Two integrations of LMDZOR allow to evaluate numerically the variation of $\Delta R$ associated with the variation of thermal inertia between high and low value, $\Delta\Gamma$. The sensitivity of the diurnal amplitude of the net radiation to the soil thermal inertia $S_{R,\Gamma}$ is then evaluated with the following equation:

$$S_{R,\Gamma} \approx \frac{1}{(\Gamma_{high}-\Gamma_{low})} \frac{\Delta R(\Gamma_{high})-\Delta R(\Gamma_{low})}{\Gamma_{inter}\sqrt{\frac{2\pi}{\tau}}+[(1-\alpha)F'_d+\alpha F'_n]} \tag{A1}$$

The map of $S_{R,\Gamma}\Delta\Gamma$ (not shown) is similar to the map of $\frac{\partial\Delta T_s}{\partial\Gamma}|_{\Delta R=cst}\Delta\Gamma$ displayed in Figure 6, but the values of $S_{R,\Gamma}\Delta\Gamma$ are positive with values less than 20% of the values of $\frac{\partial\Delta T_s}{\partial\Gamma}|_{\Delta R=cst}\Delta\Gamma$. This supports the idea that to a first-order approximation, the sensitivity of the diurnal amplitude of the net radiation to the soil thermal inertia can be neglected in the conceptual model. However, the sign of $S_{R,\Gamma}$ suggests that the conceptual

model might slightly overestimate the sensitivity of the diurnal amplitude of the temperature to the thermal inertia.

**Acknowledgements**
This work was performed using HPC resources from GENCI- [TGCC/CINES/IDRIS] (grant 2016-A0020107632) S. A. Mesbah was partly supported by the French ANR ("Investissement d'avenir") project ANR-11-RSNR-0021. The data used are listed in the references. The code and the run environment are open source (http://forge.ipsl.jussieu.fr/igcmg). Nevertheless readers interested in running LMDZOR are encouraged to contact the corresponding author for full details and latest bug fixes. We also thank two anonymous reviewers for their helpful comments on the original manuscript.

## References

Aït-Mesbah, S., Dufresne, J. L., Cheruy, F., & Hourdin, F. (2015). The role of thermal inertia in the representation of mean and diurnal range of surface temperature in semiarid and arid regions. *Geophysical Research Letters*, *42*, 7572–7580. https://doi.org/10.1002/2015GL065553

Boé, J. (2013). Modulation of soil moisture/precipitation interactions over France by large scale circulation. *Climate Dynamics*, *40*, 875–892. https://doi.org/10.1007/s00382-012-1380-6

Cheruy, F., Campoy, A., Dupont, J. C., Ducharne, A., Hourdin, F., Haeffelin, M., . . . Idelkadi, A. (2013). Combined influence of atmospheric physics and soil hydrology on the simulated meteorology at the sirta atmospheric observatory. *Climate Dynamics*, *40*, 2251–2269. https://doi.org/10.1007/s00382-012-1469-y

Coindreau, O., Hourdin, F., Haeffelin, M., Mathieu, A., & Rio, C. (2007). Assessment of physical parameterizations using a global climate model with stretchable grid and nudging. *Monthly Weather Review*, *135*(4), 1474–1489.

Comer, R. E., & Best, M. J. (2012). Revisiting glace: Understanding the role of the land surface in land atmosphere coupling. *Journal of Hydrometeorology*, *13*(6), 1704–1718. https://doi.org/10.1175/JHM-D-11-0146.1

De Rosnay, P., Polcher, J., Bruen, M., & Laval, K. (2002). Impact of a physically based soil water flow and soil-plant interaction representation for modeling large-scale land surface processes. *Journal of Geophysical Research*, *107*(D11), 4118. https://doi.org/10.1029/2001JD000634

d'Orgeval, T., Polcher, J., & de Rosnay, P. (2008). Sensitivity of the West African hydrological cycle in ORCHIDEE to infiltration processes. *Hydrology and Earth System Sciences*, *12*, 1387–1401.

Dufresne, J. L., Foujols, M. A., Denvil, S., Caubel, A., Marti, O., Aumont, O., . . . Vuichard, N. (2013). Climate change projections using the ipsl-cm5 earth system model: From cmip3 to cmip5. *Climate Dynamics*, *40*(9–10), 2123–2165.

Forster, P. M. F., & Taylor, K. E. (2006). Climate forcings and climate sensitivities diagnosed from coupled climate model integrations. *Journal of Climate*, *19*, 6181–6194. https://doi.org/10.1175/JCLI3974.1

Holtslag, A. A. M., Svensson, G., Baas, P., Basu, S., Beare, B., Beljaars, A. C. M., . . . Wiel, B. J. H. V. D. (2013). Stable atmospheric boundary layers and diurnal cycles: Challenges for weather and climate models. *Bulletin of the American Meteorological Society*, *94*(11), 1691–1706. https://doi.org/10.1175/BAMS-D-11-00187.1

Hourdin, F., Grandpeix, J. Y., Rio, C., Bony, S., Jam, A., Cheruy, F., . . . Roehrig, R. (2013). LMDZ5b: The atmospheric component of the IPSL climate model with revisited parameterizations for clouds and convection. *Climate Dynamics*, *40*(9–10), 2193–2222. https://doi.org/10.1007/s00382-012-1343-y

Kooperman, G. J., Pritchard, M. S., Ghan, S. J., Wang, M., Somerville, R. C. J., & Russell, L. M. (2012). Constraining the influence of natural variability to improve estimates of global aerosol indirect effects in a nudged version of the community atmosphere model 5. *Journal of Geophysical Research*, *117*, D23204. https://doi.org/10.1029/2012JD018588

Koster, R. D., Suarez, M. J., Higgins, R. W., & Van den Dool, H. M. (2003). Observational evidence that soil moisture variations affect precipitation. *Geophysical Research Letters*, *30*(5), 1241. https://doi.org/10.1029/2002GL016571

Krinner, G., Viovy, N., de Noblet-Ducoudré, N., Ogée, J., Polcher, J., Friedlingstein, P., . . . Prentice, I. (2005). A dynamic global vegetation model for studies of the coupled atmosphere-biosphere system. *Global Biogeochemical Cycles*, *19*, GB1015. https://doi.org/10.1029/2003GB002199

Kumar, P., Podzun, R., Hagemann, S., & Jacob, D. (2014). Impact of modified soil thermal characteristic on the simulated monsoon climate over south Asia. *Journal of Earth System Science*, *123*(1), 151–160. https://doi.org/10.1007/s12040-013-0381-0

Louis, J. F. (1979). A parametric model of vertical Eddy fluxes in the atmosphere. *Boundary-Layer Meteorology*, *17*, 187–202.

Rio, C., Grandpeix, J. Y., Hourdin, F., Guichard, F., Couvreux, F., Lafore, J. P., . . . Idelkadi, A. (2013). Control of deep convection by sub-cloud lifting processes: the ALP closure in the LMDZ5B general circulation model. *Climate Dynamics*, *40*, 2271–2292.

Rio, C., & Hourdin, F. (2008a). A thermal plume model for the convective boundary layer: representation of cumulus clouds. *Journal of Atmospheric Science*, *65*, 407–425. https://doi.org/10.1175/2007JAS2256.1

Rio, C., & Hourdin, F. (2008b). A thermal plume model for the convective boundary layer: Representation of cumulus clouds. *Journal of the Atmospheric Sciences*, *65*(2), 407–425. https://doi.org/10.1175/2007JAS2256.1

Sandu, I., Beljaars, A., Bechtold, P., Mauritsen, T., & Balsamo, G. (2013). Why is it so difficult to represent stably stratified conditions in numerical weather prediction (nwp) models? *Journal of Advances in Modeling Earth Systems*, *5*, 117–133. https://doi.org/10.1002/jame.20013

Santanello, J. A. J., Peters-Lidard, C. D., Kennedy, A., & Kumar, S. V. (2013). Diagnosing the nature of land-atmosphere coupling: A case study of dry/wet extremes in the u.s. southern great plains. *Journal of Hydrometeorology*, *14*(1), 3–24. https://doi.org/10.1175/JHM-D-12-023.1

Seneviratne, S. I., Corti, T., Davin, E. L., Hirschi, M., Jaeger, E. B., Lehner, I., . . . Teuling, A. J. (2010). Investigating soil moistureclimate interactions in a changing climate: A review. *Earth-Science Reviews*, *99*(3–4), 125– 161. https://doi.org/10.1016/j.earscirev.2010.02.004

Sterk, H. A. M., Steeneveld, G. J., & Holtslag, A. A. M. (2013). The role of snow-surface coupling, radiation, and turbulent mixing in modeling a stable boundary layer over arctic sea ice. *Journal of Geophysical Research: Atmospheres*, *118*, 1199–1217. https://doi.org/10.1002/jgrd.50158

Taylor, C. M., de Jeu, R. A. M., Guichard, F., Harris, P. P., & Dorigo, W. A. (2012). Afternoon rain more likely over drier soils. *Nature*, *4*:423–426. https://doi.org/10.1038/nature11377

Wang, F., Cheruy, F., & Dufresne, J. L. (2016). The improvement of soil thermodynamics and its effects on land surface meteorology in the IPSL climate model. *Geoscientific Model Development*, *9*(1), 363–381. https://doi.org/10.5194/gmd-9-363-2016

Wang, J., Bras, R. L., Sivandran, G., & Knox, R. G. (2010). A simple method for the estimation of thermal inertia. *Geophysical Research Letters*, *37*, L05404. https://doi.org/10.1029/2009GL041851

Yamada, T. (1983). Simulations of nocturnal drainage flows by a $q^2l$ turbulence closure model. *Journal of the Atmospheric Sciences*, *40*, 91–106.